Available online at www.sciencedirect.com
SCIENCE DIRECT®
Journal of Hydrology 279 (2003) 57–69
Journal of Hydrology
www.elsevier.com/locate/jhydrol

Estimating basin-wide hydraulic parameters of a semi-arid mountainous watershed by recession-flow analysis

Guillermo F. Mendoza, Tammo S. Steenhuis, M. Todd Walter*, J.-Yves Parlange

Department of Biological and Environmental Engineering Cornell University Ithaca, NY 14853-5701, USA

Received 26 February 2002; accepted 23 April 2003

Abstract

Insufficient sub-surface hydraulic data from watersheds often hinders design of water resources structures. This is particularly true in developing countries and in watersheds with low population densities because well-drilling to obtain the hydraulic data is expensive. The objective of this study was to evaluate the applicability of 'Brutsaert' recession flow analysis to steeper and more arid watersheds than those that were previously used. Using daily streamflow data (1962–1992), a modified version of the analysis was used to estimate the subsurface hydraulic parameters of four semi-arid, mountainous watersheds (204–764 km^2) near Oaxaca, Mexico. In this analysis, a dimensionless recession curve (DRC) was translated to best-fit observed recession flow (Q) data. The basin-wide hydraulic parameters were directly related to the magnitude of the translation used to fit the DRC to the data. One unique aspect of this study was too few high flow data to confidently fit the DRC to the data via previously published protocols. We, thus, proposed using three different approaches for translating the DRC in order to establish a range for the hydraulic parameters. Our analyses predicted a narrow range of basin-wide hydraulic parameters that were near regionally measured values and consistent within commonly published values for similar geology, suggesting that the Brutsaert method is applicable to arid, mountainous basins like those used here. This method potentially provides a cost-effective alternative to traditional geohydrological field methods for determining groundwater parameters.

Keywords: Recession flow analysis; Brutsaert; Transmissivity; Boussinesq equation; Mexico; Arid watersheds; Fractured-flow

1. Introduction

Hydraulic conductivity, specific yield, and effective aquifer depth are fundamental parameters describing subsurface hydrology and they are important inputs to physically based models. Reasonable, field-based estimates of these parameter values are often not available, especially in regions of the world with low population density. Of all the typically used hydraulic parameters, hydraulic conductivity or transmissivity is the most problematic to obtain, in part because the variability of observed values spans many more orders of magnitude than other parameters. Usually, hydraulic conductivity is unsatisfactorily estimated based on laboratory measurements, which are likely lower than in situ observations (Zecharias and Brutsaert, 1988b), or based on data collected from outside the target area.

* Corresponding author. Present address: New York City Department of Environmental Protection, Kingston, NY 12401, USA, Tel.: +1-607-255-2488; fax: +1-607-255-4080.
E-mail address: mtw5@cornell.edu (M.T. Walter).

0022-1694/03/$ - see front matter © 2003 Elsevier B.V. All rights reserved.
doi:10.1016/S0022-1694(03)00174-4

Since well-drilling to estimate hydraulic parameters is often prohibitively expensive in developing countries, determining the aquifer parameters from baseflow recession analyses is a cost-effective alternative (Zecharias and Brutseart, 1988a; Bellia et al., 1992).

Brutsaert and Nieber (1977) introduced a recession flow analysis technique based on solutions to the Boussinesq equation (Boussinesq, 1904) to indirectly estimate catchment-wide hydraulic parameters (e.g. Szilagyi, et al., 1998). The method has subsequently been expanded and further investigated by Brutsaert and several co-authors (e.g. Zecharias and Brutseart, 1988a,b; Troch et al., 1993; Brutsaert, 1994). For simplicity, it will, henceforth, be referred to as the Brutsaert method.

The Brutsaert method has been primarily applied to relatively humid, slowly draining catchments with moderate topography. Brutsaert and Nieber (1977) first demonstrated the applicability of this method in the Finger Lakes region in upstate New York. Continuing research showed that the method can be applied successfully to humid, temperate regions such as the Appalachian Plateau (Zecharias and Brutseart, 1988a,b), Belgium (Troch et al., 1993), Pennsylvania (Parlange et al., 2001), and the Philippines (Malvicini et al., 2003). Brutsaert and Lopez (1998) also successfully applied the method to a watershed in Oklahoma that was slightly less humid and more topographically flat than most investigations of this methodology. When corroborating data were available, these studies found that the Brutsaert recession flow method estimated parameters that were consistent with direct field measurements.

The objective of this study was to determine how well the Brutsaert method works in a landscape that is more arid, steeper, and geologically different than those previously studied. Specifically, historical daily streamflow records from a semi-arid, mountainous basin, located near Oaxaca, Mexico were analysed to estimate basin-wide hydraulic parameters for a fractured-rock aquifer. As in many locations, especially developing regions, rural development agencies would like to develop the water resources of this watershed but lack the necessary hydraulic information. Determining the parameters for fracture-systems is especially difficult even with resources to make traditional bore-hole measurements (Paillet et al, 1987; Wand, 1991). This study drew on aspects of the Brutsaert method from both the originally proposed method (Brutsaert and Nieber, 1977) and that recently proposed by Parlange et al. (2001), which is theoretically identical to the original method and mathematically more succinct.

2. Theory

The Brutsaert method is based on solutions of the Boussinesq equation (Boussinesq, 1903, 1904), which describes drainage from an ideal, unconfined rectangular aquifer with breadth, B, bounded below by a horizontal impermeable layer, and flowing laterally into a fully penetrating stream (Fig. 1). Brutseart and Nieber (1977) identified three theoretical solutions of the Boussinesq equation that characterize different recession flow regimes and take the following form:

$$\frac{\mathrm{d}Q}{\mathrm{d}t} = -aQ^b \tag{1}$$

where Q is recession flow [L^3T^{-1}], t is time [T], and a and b are constants for a particular recession flow regime. The parameter a is directly proportional to basin-wide groundwater parameters.

Fig. 1 conceptually illustrates how the water table changes as groundwater drains into a river, starting with a fully filled aquifer. The time period $t < t_3$ in Fig. 1 is referred to as the 'short-time' flow regime and is expected to appear in discharge data following

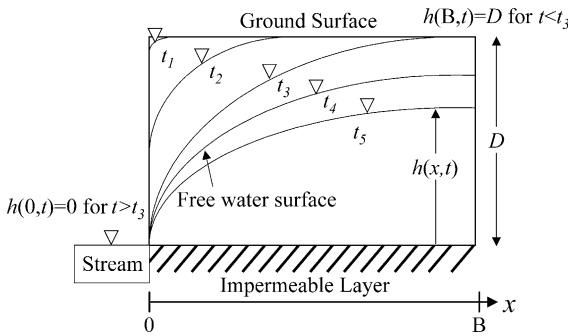

Fig. 1. The idealized, unconfined, horizontal aquifer assumed in Boussenesq's groundwater hydraulic theory with the progression of the water surface as the aquifer drains to the stream. The time, t_3, is when the recession flow transitions from the short-time regime ($t < t_3$) to the long-time ($t > t_3$) regime.

shortly after major precipitation events that recharge the aquifer. Short-time flow regimes generally have relatively high Q and $|dQ/dt|$. The short-time solution is expressed as (Polubarinova-Kochina, 1962; Brutsaert and Nieber, 1977; Parlange et al., 2001):

$$\frac{dQ}{dt} = -\frac{1.1337}{kfD^3L^2}Q^3 \tag{2}$$

where k is the saturated hydraulic conductivity [LT^{-1}], f is the drainable porosity or specific yield [-], D is the aquifer thickness [L], and L is the total length of upstream channel intercepting groundwater flow [L]. Note that b from Eq. (1) is equal to 3 for the short-time solution.

The time period $t > t_3$ in Fig. 1 is the 'long-time' flow regime and Brutsaert and Nieber (1977) showed that the associated solution to Eq. (1) for long-time recession flow can be expressed as:

$$\frac{dQ}{dt} = -\frac{4.8038k^{1/2}L}{fA^{3/2}}Q^{3/2} \tag{3}$$

where A is the upland drainage area [L^2]. Note that b from Eq. (1) is equal to 3/2 for the long-time solution.

A third solution to Eq. (1) was derived by linearizing the Boussinesq equation and is referred to as the linear solution, i.e. $b = 1$. This solution has often been employed to describe recession flow for both short- and long-times (Brutsaert and Nieber, 1977; Brutsaert, 1994; Brutsaert and Lopez, 1998; Mavicini et al., 2003):

$$\frac{dQ}{dt} = -\frac{0.3465\pi^2 kDL^2}{fA^2}Q \tag{4}$$

This linear solution is similar to the traditionally used hydrograph separation technique described by Barnes (1940) and others, and known by several names including the linear reservoir and variable slope methods.

Parlange et al. (2001) provided a single analytical formulation that gives a smooth transition between the short-time flow regime, with $b = 3$, and the long-time flows, with $b = 3/2$. This solution uses the following dimensionless definitions for flow, Q^*, and time, t^*, from the short-time solution, Eq. (2), which are applicable to the long-time solution, Eq. (3), at the transition point, e.g. $t = t_3$ in Fig. 1 (Parlange et al., 2001):

$$Q = \frac{kAD^2}{B^2}Q^*;\quad Q^* = \alpha(t^*)^{-1/2};\quad t^* = \frac{Dkt}{fB^2} \tag{5}$$

where B is the breadth of the aquifer (Fig. 1), A is the drainage area ($A = 2BL$) and $\alpha = (5-\sqrt{7})/4\sqrt{\pi} = 0.33205734$ (Parlange et al., 1981). Parlange et al. (2001) modified the linearized form of the Boussinesq equation using an analytical approximation that satisfies both the short- and long-time outflow conditions and is expressed as dimensionless cumulative outflow:

$$I^* = 2\alpha\sqrt{t^*}\left[1-\exp\left(\frac{1}{t^*}\right)\right] + \frac{5}{4}\operatorname{erfc}\left(\frac{1}{\sqrt{t^*}}\right) - \frac{1}{4}\left[\operatorname{erfc}\left(\frac{1}{\sqrt{t^*}}\right)\right]^{\sqrt{7}} \tag{6}$$

where I^* is dimensionless cumulative outflow ($\int_0^{t^*} \times Q^*(z)dz$). The transition point between the short- and long-time flow regimes is at $t^* = 0.5625$ (Parlange et al., 2001). The dimensionless outflow, $Q^* = dI^*/dt^*$, for both short- and long-time flow regimes is:

$$Q^* = \frac{\sqrt{7}\exp\left(-\frac{1}{t^*}\right)}{4\pi^{1/2}t^{*3/2}} \times \left[\frac{5t^*\exp\left(\frac{1}{t^*}\right)}{\sqrt{7}} - \operatorname{erfc}\left(\frac{1}{\sqrt{t^*}}\right)^{(\sqrt{7}-1)} + \frac{5t^*\exp\left(\frac{1}{t^*}\right)}{\sqrt{7}} - t^*\exp\left(\frac{1}{t^*}\right) + t^* + 2 - \frac{5}{\sqrt{7}}\right] \tag{7}$$

3. Theoretical assumptions and potential limitations

The groundwater hydraulic theory presented here assumes many simplifications with regard to hydrology and morphological geometry. For example, evapotranspiration (ET) and aquifer-slope are not considered. Nonetheless, applications of the theory to real watersheds show that these assumptions do not

seriously hinder the usability of the Brutseart method for determining subsurface hydraulic properties (Brutsaert and Neiber, 1977; Troch et. al, 1993; Brutsaert and Lopez, 1998; Malvicini, 2003). Although Zecharias and Brutsaert (1988a) analytically determined that average basin slope was an important morphological parameter controlling recession flow, subsequent numerical analyses (Brutsaert, 1994) and field investigations (Zecharias and Brutsaert, 1988b) have shown that the importance of slope is largely restricted to the early stages of recession flow. Specifically, Zecharias and Brutsaert (1988b) noticed that the effect of slope on recession flow was very short lived in the steep, V-shaped, unglaciated valleys of Appalachia. Additionally, Lacey and Grayson (1998) examined dimensionless slope and baseflow parameters and found no correlation between the two for small watersheds ($A < 40$ km^2) of similar geology-vegetation types.

Studies show that the theory is applicable across a wide range of system complexity. Szilagyi and Parlange (1998) used the basic theory presented here to analyse synthetic watersheds of varying complexity with predefined hydraulic parameters and they found that increasing the watershed complexity had minimal effect on the estimations of the hydraulic parameters. Furthermore, Zecharias and Brutsaert (1988b) found that the effect of ET is negligible since it is mostly limited to riparian zones along stream channels. In short, field observations and other investigations largely confirm that the theory's simplifications in basin geometry and hydrological processes are not seriously problematic to the real-world application of the Brutsaert method. However, the theory has only been field-tested in humid, topographically moderate regions.

The theory still requires fieldwork to understand its applicability to a broader range of real systems. Some studies have shown long-time flows to be best characterized by Eq. (3) ($b = 1.5$), (Brutsaert and Nieber, 1977; Troch et al., 1993; Parlange et al., 2001) and other studies have found the linear solution, Eq. (4), ($b = 1$) to work best (Brutsaert and Lopez, 1998; Malvicini et al., 2003). Malvicini et al. (2003) suggest that the integration of sub-basins with different response times may be more important for determining the long-time solution that best describes the recession data than the match between basin morphology and the theory. Also interesting, Brutsaert and Lopez (1998) found that their estimates of k for 22 central Oklahoma sub-basins were slightly negatively correlated with basin size and it is unclear why. Moreover, all the studies cited here are based on data that contains both short- and long-time recession flow regimes. In this study, we tested how well the Brutsaert method works for a complex watershed with steep, fractured-bedrock in a semi-arid climate, and very little short-time recession flow data.

4. Location and methods

4.1. Site description

The study was carried out in the Yosocuta Watershed of the Mixteca River near Oaxaca, Mexico (97°40′W, 17°55′N), which drains a semi-arid mountain range in a region called the Mixteca Alta or Sierra de Zapotitlan, an extension of the Southern Sierra Madre. Average daily streamflow data for four gage stations in the watershed were obtained from the Mexican National Water Commission (CNA); sub-daily data were unavailable. The stations were La Junta, Camotlan, Yundoo, and Xatan (Table 1, Fig. 2). La Junta is near the base of the Yosocuta Watershed just before it enters the reservoir and encompasses the sub-basins of the other three stations. Typically ~25% of each watershed's area has slopes above 18° (Fig. 2). Annual rainfall is ~700 mm; La Junta receives 654 mm and Camotlan 780 mm. Perennial contact springs and continuous baseflow sustain the streams in these watersheds. The watersheds have generally increasing flows in the downstream direction.

The geology of the Yosocuta Watershed is largely the result of volcanic activity and intense erosion (Torales Iniesta, 1998). Eroded rock has created sedimentary deposits, many of which have consolidated and encapsulated igneous intrusions of basalt and andesite. Tectonic movements and climate changes created a ubiquitous network of fissures, faults, and fractures in the rock. A thin layer of soil, typically <10 cm thick, sparsely covers the hillsides, whereas the valley bottoms consist of more deeply accumulated soil deposits. Irrigated farming takes place on the valley bottoms. Most creeks have

Table 1
Watershed characteristics

Gauging station (CNA ID number)	Period	Area (km^2)	Min and Max elevation (masl)	Latitude, longitude	Stream length (km)	Flow measurement method
La Junta (#18485)	1969–'1992	764	1541–2886	97°47′06″, 17°47′09″	321	Continuous, automatic[a]
Camotlan (#18337)	1963–1969	255	1760–2886	97°41′15″, 17°54′30″	114	Daily, manual[b]
Xatan (#18338)	1963–'1967	211	1670–2576	97°42′00″, 17°47′00″	88	Continuous, automatic[a]
Yundoo (#18573)	1979–'1988	204	1778–2886	97°47′00″, 17°57′09″	92	Daily, manual[c]

[a] Stage measured with a Rossbach IV #735, stream reach is straight for 180–200 m with high rock banks, flow measured regularly from a cable using a Rossbach #61605 impellor.
[b] Manually read staff is attached to bridge abutment, flow measured regularly by wading with a Price meter.
[c] Manually read staff secured above a wier, flow measured regularly by wading with a Price meter.

perennial baseflow originating from fractures, faults and fissures in the mountainsides.

The water in the rock has been traditionally tapped by systems called *galerias filtrantes*, which are a network of subterranean tunnels that intercept springs. These systems are found on the gently sloped eastern side of the range along the Tehuacan Valley. Galerias filtrantes are believed to have originated in Persia where they are called *qanats* and were introduced to Eurpoeans around 1500 AD and brought to the New World by the Spanish Conquistadors. These tunnels average 2.2 km into the rock and, in 1978, 129 galerias filtrantes irrigated 16,539 ha (Enge and Whiteford, 1989). Farmers in the Yosocuta Watershed rely exclusively on base-flow water to irrigate their crops throughout the dry

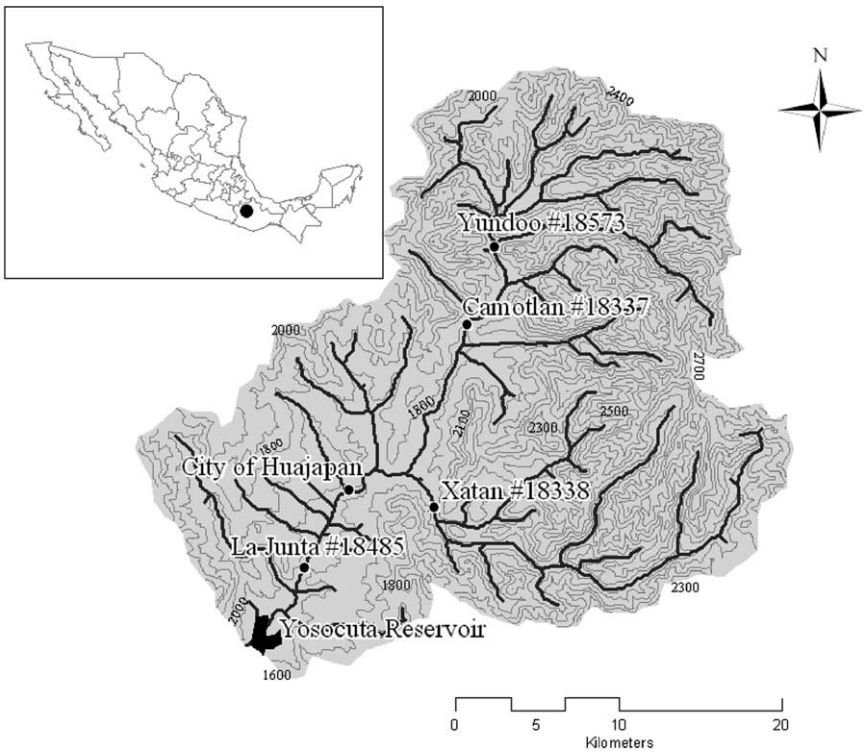

Fig. 2. Elevation map of the Yosocuta Watershed, the locations of the stream gauges, and the sub-basin boundaries associated with each gauge.

season, often constructing simple galerias filtrantes by laying perforated pipe underneath the streambed gravel.

The Yosocuta Watershed is a major source of the 46.8×10^6 m^3 Yosocuta Reservoir, which supplies water to the city of Huajuapan de Leon (1993 pop. $>$ 100,000) and a 2000 ha irrigation district called San Marcos Arteaga-Tonala-Los Nuchitas. The irrigation district is allocated 20×10^6 m^3 yr^{-1} and the growing city of Huajuapan is allocated 1.31×10^6 m^3 yr^{-1} (Garcia Blanco et al., 1993). Despite the importance of continued water resource development, hydraulic conductivity, effective aquifer depth, and specific yield are unknown for the Yosocuta Watershed. The closest relevant data are transmissivity values (2.9×10^3 and 393×10^3 m^2 s^{-1}) were determined with pumping well tests for a fractured rock region in the Chalco Watershed, ~200 km from the study site, (Bellia et al., 1992), however, these are probably overestimates (Huntley et al., 1992).

4.2. Recession flow analysis

Streamflow recession records were selected in a way that minimized the occurrence of overland flow and insured only baseflow. Given the rapid response of the watershed, this was achieved by excluding all rising limb data and data that coincided with observed rainfall at the weather stations located at La Junta and Camotlan. Only data showing 2 or more consecutive days of recession were included. Following the approach of Brutsaert and Lopez (1998) in analysing recession flow data, it was convenient to plot the data as $\log(|dQ/dt|)$ vs. $\log(Q)$ for each watershed using $\log(|dQ/dt|) \approx \log[(Q_i - Q_{i-1})/dt]$ vs. $\log(Q) \approx \log[(Q_i + Q_{i1})/2]$ where i represents a discrete data point and dt is the time between two points. This log transformation greatly simplifies the analysis in part because the theoretical relationship, Eq. (1), becomes linear: i.e. $\log(|dQ/dt|) = b\log(Q) + \log(a)$.

Basin-wide hydraulic parameters were estimated by translating the theoretical curve described by Parlange et al. (2001), i.e. based on Eq. (7), to observed data as shown in Fig. 3. The translation magnitudes in the horizontal or abscissa [$\log(Q)$] and vertical or ordinate [$\log(|dQ/dt|)$] directions, i.e. H and V, respectively (Fig. 3), can be related to

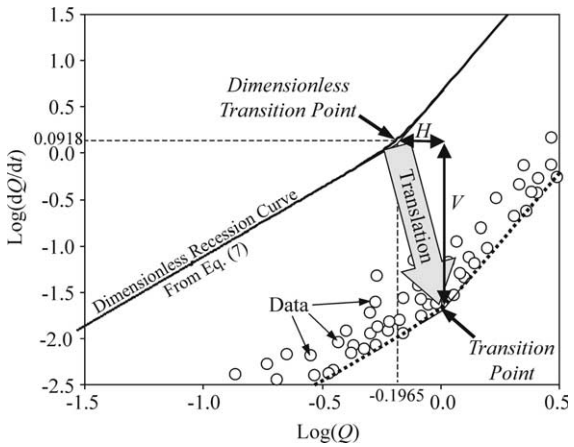

Fig. 3. A schematic showing how the dimensionless curve of $\log(|dQ^*/dt^*|)$ vs. $\log(Q^*)$ from Eq. (7) (solid line) is translated to correspond with data (symbols). The dashed line shows the translated curve. Also identified are the 'dimensionless transition point,' the observed 'transition point,' the magnitude of vertical translation, V, and the magnitude of horizontal translation, H.

the basin-wide parameters as follows (Parlange et al., 2001):

$$H = \frac{kAD^2}{B^2} \tag{8a}$$

$$V = \frac{k^2AD^3}{fB^4} \tag{8b}$$

There are three probable unknown hydraulic parameters, k, D, and f, and two equations so it was necessary to make reasonable estimates of one of the three parameters. Typically, guesses are best made for drainable porosity, f, because of the narrower range of published data. Transmissivity, $T = kD$, and aquifer depth, D, can then be estimated as functions of drainable porosity, f :

$$T = \frac{V}{H} fB^2 \tag{9}$$

$$D = \frac{H^2}{V}\frac{1}{fA} \tag{10}$$

where $B = 2L/A$, L is the total length of stream channel, and A is the watershed area.

5. Results

Figs. 4–7 are graphs of $\log(|dQ/dt|)$ vs. $\log(Q)$ for the four catchments, Yundoo, Camotlan, Xatan, and

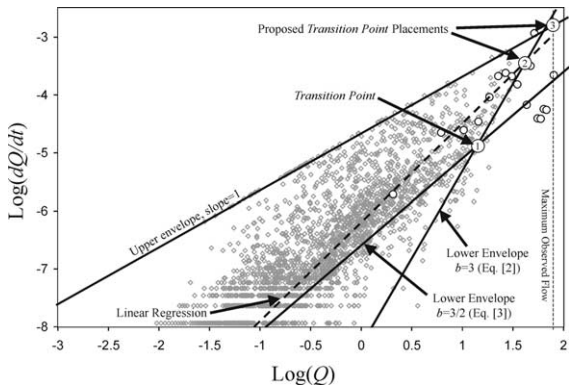

Fig. 4. Recession flow data from La Junta. The large symbols are the averages within each flow interval. The dashed line represents the linear regression of the flow averages. The top line is the 1:1 envelope, the two bottom lines are the $b = 3/2$ and $b = 3$ lower envelopes, as labeled. The numbered points are the location of the three *transition point* placement methods, respectively.

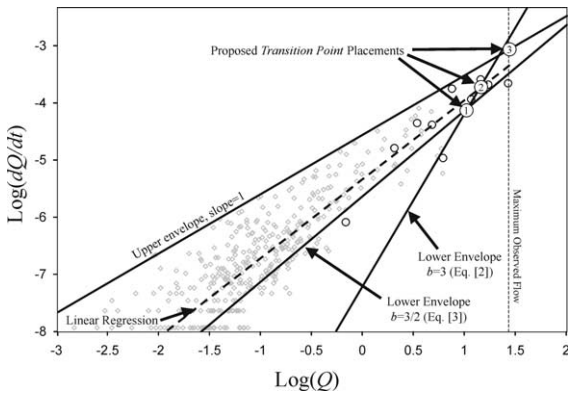

Fig. 6. Recession flow data from Xatan. The large symbols are the averages within each flow interval. The dashed line represents the linear regression of the flow averages. The top line is the 1:1 envelope, the two bottom lines are the $b = 3/2$ and $b = 3$ lower envelopes, as labeled. The numbered points are the location of the three *transition point* placement methods, respectively.

La Junta, respectively. As expected, the highest recession flow, 81 $m^3 s^{-1}$, was observed from the largest basin, La Junta. Since the periods of record do not completely coincide (Table 1), maximum observed recession flow did not directly nor consistently correlate to basin size. For example, Yundoo, the smallest basin, had the second highest flow (29 $m^3 s^{-1}$), higher even than Camotlan (13 $m^3 s^{-1}$) which encompassed Yundoo. The horizontal stratification at lower flows is a consequence of the precision of the streamflow measurements and is also evident in previous studies (e.g. Brutseart and Nieber, 1977; Parlange et al., 2001).

When both flow regions are represented in the data, Barnes (1940) proposed that short- and long-time flow regimes visually manifest themselves in the shape of the 'lower envelope' of log–log plotted data; i.e. a break in the slope of a line enveloping the lower boundary of the $\log(|dQ/dt|)$ vs. $\log(Q)$ data indicates a *transition point* between short- and long-time flow with slopes of 1:1.5 and 1:3, respectively; this is showed in Fig. 3. The clearest

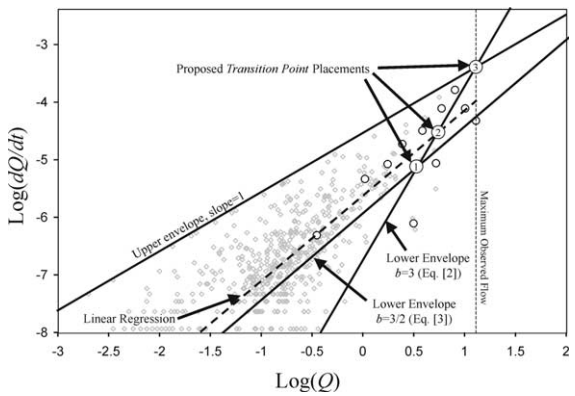

Fig. 5. Recession flow data from Camotlan. The large symbols are the averages within each flow interval. The dashed line represents the linear regression of the flow averages. The top line is the 1:1 envelope, the two bottom lines are the $b = 3/2$ and $b = 3$ lower envelopes, as labeled. The numbered points are the location of the three *transition point* placement methods, respectively.

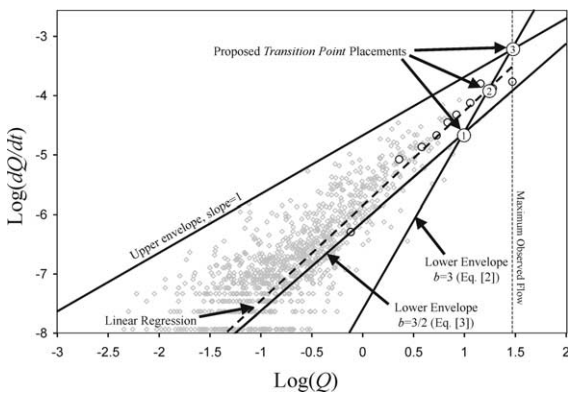

Fig. 7. Recession flow data from Yundoo. The large symbols are the averages within each flow interval. The dashed line represents the linear regression of the flow averages. The top line is the 1:1 envelope, the two bottom lines are the $b = 3/2$ and $b = 3$ lower envelopes, as labeled. The numbered points are the location of the three *transition point* placement methods, respectively.

transition point among these data was for La Junta, the largest, all-encompassing watershed; note the 'lower envelope' lines, with slopes 1:1.5 (long-time regime) and 1:3 (short-time regime) in Fig. 4, corresponding to Eqs. (3) and (2), respectively. The 'lower envelope' lies below 90% of the data (Brutsaert and Nieber, 1977). No similar obvious breaks in the slope of the lower envelope of the data were apparent for the small watersheds (Figs. 5–7). We expected that only the long-time flow regime would be exhibited because short-time flow probably occurred within two days of rainfall events and these were necessarily excluded from the analysis. Given that both short- and long-time flow regimes cannot be confidently identified in the recession flow data, it is not immediately clear how to use the methodologies described by Brutsaert and Nieber (1977) or Parlange et al. (2001).

To verify that long-time flow alone is indeed exhibited Figs. 5–7, a linear regression was performed on the $\log(|dQ/dt|)$ vs. $\log(Q)$ recession flow data (dashed lines in Figs. 4–7). The slope of the regressions provides insight into the average basin-wide recession constant, b, which helps identify the dominant flow regimes. In accordance with Parlange et al. (2001), the recession flows were divided into 20 equal flow intervals in order to avoid potential biased regression analysis due to the skewed data distribution. Within each interval, an average $\log(|dQ/dt|)$ was estimated, and the linear regression was applied to these averages. The flow intervals used were 4.00, 1.39, 0.69, and 1.58 $m^3 s^{-1}$ for La Junta, Xatan, Camotlan, and Yundoo, respectively. The large open circles in Figs. 4–7 represent the mean values of Q and $|dQ/dt|$ within each flow interval; note that the increments represented by each average point do not appear equal because the flow data were log transformed. In some cases there were less than 20 mean points because no points fell within some intervals, especially at high flows. Table 2 shows that the regression slopes were $b \sim 3/2$, i.e. consistent with b in Eq. (3), reinforcing our conclusion that long-time flow dominated the data in Figs. 5–7. For the La Junta data (Fig. 4), the linear regression was limited to the lower ten average recession flow points (open circles) because the upper ten points were clearly in the short-time regime and showed excessive scatter due to a relatively small amount of data in some flow increments. La Junta's regression line slope was 1.7 (Table 2), i.e. between the theoretical slopes 1.5 (Eq. (3)) and 3 (Eq. (2)), which suggests that some of the data included in the regression lie in the short-time regime (Fig. 4). In other words, data below the transition point should theoretically show a 1:1.5 slope (Parlange et al., 2001) and data above the transition point should show a slope of 1:3, thus, because our La Junta regression included data from both regimes, our regression slope is between the theoretical slopes.

Unlike previously published studies for which data exhibited both short- and long-time flow regimes, we cannot use statistics to best-fit Eq. (7) (Parlange et al., 2001) or Eqs. (2)–(4) (e.g. Brutsaert and Nieber (1977)) to envelop the data because we have too-few short-time recession data. Instead, we propose fitting Eq. (7) by estimating the location of transition point among the log-plotted data and translating the theoretical curve so that the *dimensionless transition point* and observed transition point match (Fig. 3). In short, the dimensionless values, Q^* and dQ^*/dt^*, from

Table 2
Results from the linear regression of watershed response averages and placements of change of flow regime points

	Slope of linear regression (R^2)	Intercept of 1:1 upper boundary line	Coordinates of flow regime transition point: $\log(Q)$, $\log(\lvert dQ/dt\rvert)$		
			Placements		
			1	2	3
La Junta	1.7 (0.93)	−4.64	1.91, −2.73	1.81, −3.08	1.25, −4.76
Camotlan	1.4 (0.63)	−4.64	1.11, −3.52	0.85, −4.42	0.57, −5.23
Xatan	1.5 (0.82)	−4.64	1.42, −3.21	1.13, −3.82	1.01, −4.18
Yundoo	1.6 (0.96)	−4.64	1.47, −3.17	1.11, −4.07	0.82, −4.94

Eq. (7) are translated in the horizontal, H, and vertical, V, directions to fit observed data using only the flow regime transition point to fit the theory to the data (Fig. 3).

The theoretical or dimensionless transition point was determined from Eq. (7) by locating the intersection of the short- and long-time asymptotes above and below $t^* = 0.5625$, respectively. Using least squares optimization, the intercept of these asymptotes is at $\log(Q^*) = -0.1965$ and $\log(|dQ^*/dt|) = 0.0918$ (Fig. 3). To verify these coordinates, we substituted the relationships in Eq. (5) into Eqs. (2) and (3) solved the two equations simultaneously and found the *dimensionless flow transition point* at $\log(Q^*) = -0.1839$ and $\log(|dQ/dt|) = 0.1048$, which is similar to the previous result.

As mentioned earlier, locating the actual transition point among the measured data was not obvious so we proposed three methods for identifying transition points that bracket or place boundaries on the actual transition point. For each watershed, we located three possible transition points, noted as (1), (2), and (3) in Figs. 4–7, using the following three placement strategies:

(1) This placement utilized the methodology originally proposed by Brutsaert and Nieber (1977) in which a lower envelope of the data was delineated by short- and long-time recession Eqs. (2) ($b = 3$) and (3) ($b = 3/2$), respectively. Each equation was fitted to the data such that 90% of the data lie above and to the left of the envelope defined by Eqs. (2) and (3); these are the solid 'lower envelope' lines in Figs. 4–7. The intersection of these two resulting lines identifies the flow transition point and is labeled as (1) in Figs. 4–7. This transition point probably lies too low on the $\log(Q)$ vs. $\log(|dQ/dt|)$ plot due to the lack of short-time data (Figs. 5–7) and thus this placement represents a lower boundary for the transition point.

(2) This placement was the intersection of the regression line through the averages of the flow intervals, i.e. the dashed line in Figs. 4–7, with the line in Figs. 4–7 that indicates the 'lower envelope $b = 3$ (Eq. (2))'. This placement is similar to that used by Parlange et al. (2001) and represents an intermediate placement on the $\log(Q)$ vs. $\log(|dQ/dt|)$ plot (Figs. 5–7). This placement is labeled (2) on Figs. 4–7.

(3) This placement of the flow transition point was the intersection between a 1:1 line enveloping the upper boundary of the data (solid 'upper envelop' line in Figs. 4–7) with a line indicating the upper extent of the observed $\log(Q)$ data (vertical dashed line in Figs. 4–7). A 1:1 upper envelope has been observed in many studies (Troch et al., 1993; Brutsaert and Lopez, 1998; Brutsaert and Nieber, 1977; Parlange et al., 2001) but it has not been discussed. This placement attempted to identify the highest probable recession flow and was expected to set an upper boundary for the flow transition point. This placement is labeled as (3) in Figs. 4–7.

The numbered circles in Figs. 4–7 indicate the transition points, as obtained by each of the above methods; the numbers correspond to the description numbers above. The differences among the flow transition point placement using these three approaches and the dimensionless transition point [$\log(Q) = -0.1965$, $\log(|dQ/dt|) = 0.0918$] were used to determine H and V translations and, ultimately, basin-wide transmissivity and depth using Eqs. (9) and (10).

Placement (1), from Brutsaert and Nieber (1977), was easily applied to the La Junta Watershed because the transition point between short- and long-time flow regimes was relatively easily identified (Fig. 4). Placements (2) and (3) were also used on LaJunta to test the method's sensitivity to transition flow point placement (Fig. 4). Figs. 5–7 show the three placement-strategies applied to the small watersheds that lacked adequate short-time flow data. Table 3 shows the horizontal and vertical translations, H, and V for each placement on each watershed.

Figs. 8 and 9 show estimated hydraulic parameters, T and D, respectively, for each watershed over a range of possible f using Eqs. (9) and (10) and the H and V values in Table 3. As discussed earlier, the drainable porosity, f, generally exhibits a smaller, more predictable range of values than the other groundwater parameters and thus we solved the others based on estimates of f. A drainable porosity, f, between 0.0001 and 0.001 was our best estimate based on measurement is similar types of material (Gordon,

Table 3
Values for the horizontal, H, and vertical, V, translations for each placement strategy and each basin; the values define the relationships between aquifer depth, D, specific yield, f, and hydraulic conductivity, k

	$H(m^3\ s^{-1})$ Placements			$V(10^{-5} \times m^3\ s^{-1}\ d^{-1})$ Placements		
	1	2	3	1	2	3
La Junta	27.7	100.4	127.6	1.41	66.6	152.3
Camotlan	5.81	11.1	20.4	0.47	3.17	24.3
Xatan	15.96	21	41.7	5.45	12.3	49.7
Yundoo	8.9	17.2	46.1	0.73	5.32	54.4

1986; Moore, 1992) and following fracture-flow theory (e.g. Maini and Hacking, 1977; Larsson, 1997). This range is in the middle of the textbook range of f for fractured rock (e.g. Freeze and Cherry, 1979). The estimated T and D values were relatively consistent among the different catchments despite the fact that their sizes were different and the study region was assumed to be highly variable due to the fractured bedrock, uneven topography, and spatially heterogeneous rainfall patterns. For any given f, the range of estimated T among the basins was within one order of magnitude (Fig. 8), and at low f the absolute range in

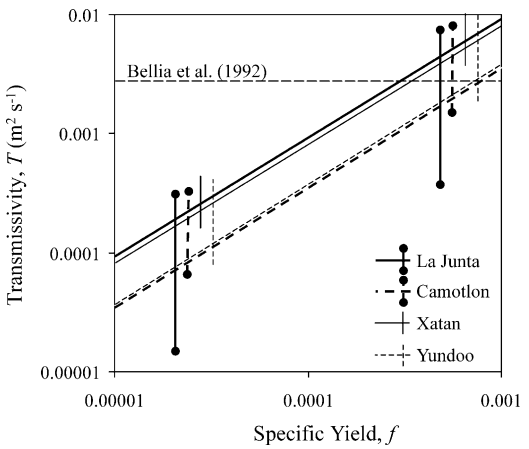

Fig. 8. Plot of transmissivity, $T = kD$, vs. specific yield, f, for all catchments and *transition point* placement methods. Each line shows the results using *transition point* placement (2) for a specific catchment, the upper error bars shows results using placement (3) and the lower error bar corresponds to placement (1). The horizontal dashed line corresponds to the low-end T measured by Bellia et al. (1992).

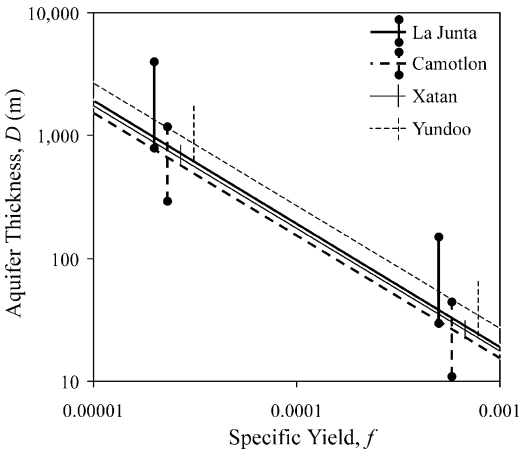

Fig. 9. Plot of aquifer thickness, D, vs. specific yield, f, for all catchments and *transition point* placement methods. Each line shows the results using *transition point* placement (2) for a specific catchment, the upper error bars shows results using placement (1) and the lower error bar corresponds to placement (3).

estimated T is small. The lowest extent of the error bars in Fig. 8 corresponds to estimates made using placement (1) and the highest corresponds to placement (3). In contrast to Fig. 8, the lowest extent of the error bars in Fig. 9 corresponds to placement (3) and the upper for placement (1). Placement (2) always resulted in intermediate parameter values, shown as the primary trend lines in Figs. 8 and 9.

6. Discussion

Although the data in Figs. 4–7 are highly scattered, the $\log(|dQ/dt|)$ vs. $\log(Q)$ relationships for all the watersheds are generally similar, as the theory would predict; i.e. groundwater characteristics for nearby watersheds should be similar. For example, all the watersheds exhibited long-time flow that was characterized by $b = 3/2$. This flow characteristic that had been observed for long-time flow data from much more humid, gently sloping watershed and now has been duplicated for these semi-arid, mountainous watersheds. Our results support Zecharias and Brutsaert (1988b) conclusion that basin geomorphology is a more significant control on recession flow characteristics than climate. The similarity in recession flow characteristics between the relatively flat or rolling watersheds studied previously and these steep

watersheds supports the theory that slope does not substantially control long-time recession flow behavior, even in very steep basins like these in Mexico for which the theoretical assumptions appear to be violated. It is interesting that the characteristic trends in basin parameters with respect to watershed size observed by Zecharias and Brutsaert (1988a) were not evident in these systems.

The similarity in the 1:1 'upper envelopes' among the four watersheds was unexpected (Figs. 4–7) and the theory does not, in any obvious way, suggest what this boundary should look like. The line is identical for all four watersheds, with a y-intercept of −4.64 (Table 2). Although distinct 1:1 upper envelopes have been observed in other watersheds as well (Malvicini, 2003; Brutsaert and Lopez, 1998; Troch et. al, 1993), they have not been widely discussed. We hypothesize that the 1:1 line might represent some maximum physical limit of the contributing aquifer on otherwise random-like recession flow behavior.

The estimates of transmissivity are generally lower than Bellia et al. (1992) field measurements, which were $>0.0029\ m^2\ s^{-1}$ (Fig. 8), but, again, these measurements are most likely high (Huntley et al., 1992). Note that the results for the three basins for which we needed to estimate the transition point are similar to those for La Junta, the basin for which we are confident of our transition point placement. This indicates that the methods we used to estimate transition points gave good results. La Junta, for which we directly applied the Barnes (1940) method, i.e. placement (1), showed the most variability in parameter estimates among the three transition point placements, suggesting that our confidence in T and D estimates are +/− a factor of ~5 (Figs. 8 and 9).

Ten-fold variations in f corresponded to ten-fold variations in T (Fig. 8). Fig. 9 shows a similar relationship between f and D, with slightly less variability among watersheds. Xatan shows uniquely less overall variability among placements (Figs. 8 and 9). Interestingly, both T and D estimates for Camotlan were consistently lower than estimates obtained from data of the other catchments, which agrees with the relatively lower recession flow for this basin discussed earlier and suggests unique parameters among the basins. We assumed that placement (2) was our best estimate with placements (1) and (3) providing measures of uncertainty in our parameter estimations.

Because of the ubiquity of contact springs, typically shallow wells in the region (~10 m) and the emergence of perennial rivers within ~100 m of watershed divides (Fig. 2), it is unlikely that D exceeds 100 m. Similar Ds have been observed in other fractured rock systems (Paillet et al., 1987; Bayuk, 1989; Oxtobee and Novakowski, 2003). Using placement (2) and assuming this limitation on D, i.e. <100 m, we refined our range of f to 0.0015–0.001 (Fig. 9). From Fig. 8, then, the range of T is between 0.004 and $0.01\ m^2\ s^{-1}$, which translates into k between 4×10^{-5} and $1\times10^{-4}\ m\ s^{-1}$. The estimated T are higher than T for fractured media measured by Moore (1992), lower than those made by Paillet et al. (1987), and near the low end measurements made near-by by Bellia et al. (1992), which we noted earlier were probably overestimated (Huntley et al., 1992). Incidentally, the range of T estimated by the Brutsaert method, ~3 orders of magnitude, is similar to Bellia et al.'s (1992) range, ~3 orders of magnitude, which suggests that this method does not introduce more uncertainty into parameter estimates than more costly direct measures. Saturated hydraulic conductivity estimates were within a factor of three and in the middle of the published range for permeable basalt (Freeze and Cherry, 1979). The Brutsaert method allowed us to substantially refine and reduce the range of probable k relative to the generic, multiple order-of-magnitude range commonly published in text and reference books. Figs. 8 and 9 also provide specific families of values for each catchment.

7. Conclusion

Although the Brutsaert recession flow method's theoretical basis assumes an idealized horizontal aquifer (Fig. 1) and does not account for ET, it was successfully applied to the steep, fractured bedrock, semi-arid landscape of the Mixteca region in Mexico. The Brutsaert method provided a rubric for substantially refining the range of probable values for basin-wide hydraulic parameters. The estimated parameters were generally consistent with regional field measurements. For example, the predicted T, $0.001–0.0004\ m^2\ s^{-1}$, overlapped on the low side with Bellia et al.'s (1992) measurements, 0.39 and

0.0029 $m^2 s^{-1}$, which are almost certainly overestimated according to Huntley et al. (1992). This demonstrates the practical applicability of this theory to semi-arid, shallow-soil, mountainous systems, which are geologically different from the humid, gently sloping systems to which the method has been previously applied. The success of this method to predict groundwater hydraulic parameters that are consistent with field measurements, despite the arid and mountainous conditions, which appear to violate the method's theory, supports previous conclusions that recession flow behavior is not substantially dependent on ET and land slope (Zecharias and Brutsaert, 1988b).

This investigation was unique among similar studies in that short-time recession flows were not obvious for most of the study watersheds. The three approaches proposed to overcome this deficiency in the data resulted in reasonable estimates of basin-wide hydraulic parameters when compared to field observations, published values, and results from a basin for which both flow regimes were identifiable, i.e. the La Junta watershed.

This study provided continued development of a potentially useful method for estimating hydraulic parameters when there is very limited information about a catchment and an alternative approach for estimating effective hydraulic parameters for fractured-rock aquifers, for which direct measurements are not trivial. In short, this type of analysis provides a narrow range of values within the enormous range of published hydraulic parameters.

Acknowledgements

The authors would like to thank Dr Geoff Lacy (University of Melbourne, Australia) for his insights and assistance in interpreting and meaningfully presenting our results.

References

Barnes, B.S., 1940. Discussion on analysis of run-off characteristics by O.H. Meyer. Trans. Civil Eng. 21, 620–627.

Bayuk, D.S., 1989. Hydrogeology of the Lower Hayes Creek Drainage Basin, Western Montana, MS thesis University of Montana, p. 230.

Bellia, S., Cusimano, G., Gonzalez, T.M., Rodriguez, R., Guinta, G., 1992. El valle de Mexico: Consideraciones preliminares sobre los riegos geologicos y analisis hidreologico de la cuenca de Chalco. Instituto Italo-Latino Americano. Quaderni IILA. Serie Scienza 3. Roma.

Boussinesq, J., 1903. Sur le débit, en temps de sécheresse, d'une source alimentée par une nappe d'eaux d'infiltration. C.R. Hebd Sé-ances Acad. Sci. 136, 1511–1517.

Boussinesq, J., 1904. Recherches theoriques sur l'ecoulement des nappes d'eau infiltrees dans le sol et sur le debit des sources. J. Math. Pures Appl. 5me. Ser. 10, 5–78.

Brutsaert, W., 1994. The unit response of groundwater outflow from a hillslope. Water Resour. Res. 30 (10), 2759–2763.

Brutsaert, W., Nieber, J.L., 1977. Regionalized drought flow hydrographs from a mature glaciated plateau. Water Resour. Res. 3 (3), 637–643.

Brutsaert, W., Lopez, J.P., 1998. Basin-scale geohydrologic drought flow features of riparian aquifers in the southern great plains. Water Resour. Res. 34 (2), 233–240.

Enge, K.I., Whiteford, S., 1989. The Keepers of Water and Earth: Mexican rural social organization and irrigation, University of Texas Press, Austin, p. 222.

Freeze, R.A., Cherry, J.A., 1979. Groundwater, Prentice-Hall, Englewood Cliffs, NJ, p. 604.

Garcia Blanco, J.M., Martinez Ramirez, S., Hernandez Aquino, F., 1993. Consideraciones preliminares sobre la situacion de la presa Yosocuta y su cuenca de alimentacion. Temas. Universidad Tecnologica de la Mixteca, 17–31.

Gordon, M.J., 1986. Dependence of effective porosity on fractured continuity in fractured media. Ground Water 24 (4), 446–452.

Huntley, D., Nommensen, R., Steffey, D., 1992. The use of specific capacity to assess transmissivity in fractured-rock aquifers. Ground Water 30 (3), 396–402.

Lacey, G.C., Grayson, R.B., 1998. Relating baseflow to catchment properties in south-eastern Australia. J. Hydrol. 204, 231–250.

Larsson, E., 1997. Groundwater flow through a natural fracture. Flow experiments and numerical modeling: Flow experiments and Numerical Modelling. Lic-Thesis. Dept. of Geology. Chalmers University of Technology. Göteborg, Sweden.

Maini, T., Hacking, G., 1977. An examination of feasibility of hydrologic isolation of a high level waste repository in crystalline rocks. Invited paper, Geologic Disposal of High Radioactive Waste Session, Ann. Meeting, Geol. Soc. Am., Seattle, Washington.

Malvicini, C.F., Steenhuis, T.S., Walter, M.T., Walter, M.F., 2003. Evaluation of spring flow in the uplands of Matalom, Leyte, Philippines. Adv. Water Resour. 2003 (accepted for publications).

Moore, G.K., 1992. Hydrograph analysis in a fractured rock terrane. Ground Water 30 (3), 390–395.

Oxtobee, J.P.A., Novakowski, K., 2003. A field investigation of groundwater/surface water interaction in a fractured bedrock environment. J. Hydrol. 269 (3-4), 169-193.

Paillet, F.L., Hess, A.E., Cheng, C.H., Hardin, E., 1987. Characterization of fracture permeability with high-resolution flow measurements during borehole pumping. Ground Water 25 (1), 28–40.

Parlange, J.-Y., Braddock, R.D., Sander, G., 1981. Analytical approximation to the solution of the Blasius equation. Acta Mechanica 38, 119–125.

Parlange, J.-Y., Stagnitti, F., Heilig, A., Szilagyi, J., Parlange, M.B., Steenhuis, T.S., Hogarth, W.L., Barry, D.A., Li, L., 2001. Sudden drawdown and drainage of a horizontal aquifer. Water Resour. Res. 37 (8), 2097–2101.

Polubarinova-Kochina, P.Y.-A., 1962. In: DeWiest, R.J.M, (Ed.), Theory of Groundwater Movement, translated from russian, Princeton University Press, Princeton, NJ, p. 613.

Szilagyi, J., Parlange, M.B., 1998. Baseflow separation based on analytical solutions of the Boussinesq equation. J. Hydrol. 204, 251–260.

Szilagyi, J., Parlange, M.B., Albertson, J.D., 1998. Recession flow analysis for aquifer parameter determination. Water Resour. Res. 34 (7), 1851–1857.

Torales Iniesta, J.S., 1998. Informacion historica de las rocas de Oaxaca. Temas de Ciencia y Tecnologia. Universidad Tecnologica de la Mixteca 2 (6), 21–28.

Troch, P.A., De Troch, F.P., Brutsaert, W., 1993. Effective water table depth to describe initial conditions prior to storm rainfall in humid regions. Water Resour. Res. 29 (2), 427–434.

Wand, J.S.Y., 1991. Flow and transport in fractured rocks. US National Report to International Union of Geodesy and Geophysics. Rev. Geophys., Supp. April, 254–262.

Zecharias, Y.B., Brutsaert, W., 1988a. The influence of basin morphology on groundwater outflow. Water Resour. Res. (10), 1645–1650.

Zecharias, Y.B., Brutsaert, W., 1988b. Recession characteristics of groundwater outflow and baseflow from mountainous watersheds. Water Resour. Res. 24 (10), 1651–1658.